

# Periodic Oscillation and Fine Structure of Wedge-Induced Oblique Detonation Waves

Mingyue Gui, Baochun Fan, Zhihua Chen

State Key Laboratory of Transient Physics, Nanjing University of Science and Technology,  
Nanjing, Jiangsu 210094, China

## 1 Introduction

Oblique detonation wave stabilized over a body has been studied due to the ongoing development of high-speed propulsion systems, such as ODW engines and ram accelerators.

Experimental observations by Lehr [1], Dabora et al [2], Viguier et al [3,4], Kamel et al [5], and Morris et al [6] show that at least two different kinds of overall flow configurations involving standing oblique detonation waves by the wedge are observed. The first is a direct initiation of a detonation wave at the wedge surface. The second possibility is an oblique shock wave/oblique detonation wave (OSW/ODW) transition which occurs at a certain distance from the apex of the wedge.

Numerical simulations of wedge-induced detonations conducted by many authors [7-9] have been showed that a standing oblique detonation is stable even in the presence of very strong perturbations. Recently Choi et al [10] captured numerically the unsteadiness ODW frontal structure. They showed that the ODW instability has a strong dependence on the activation energy. However, only single-sided triple point was found. Later Choi et al [11] analyzed ODW structure with the flow turning angle varying from  $35^{\circ}$ ~ $38^{\circ}$  and thought that flow turning angle was a key parameter for the onset condition of the dual-headed triple point structures.

In this study, an oblique detonation wave induced by a long enough wedge is numerically analyzed by high resolution algorithm. The front of an oblique detonation wave divided into three sections according to the flow field structures and oscillation features has been discussed numerically in detail.

## 2 Physical model and numerical method

The two-dimensional Euler equations with a chemical reaction in non-dimensional form are given as

$$\frac{\partial}{\partial t} \begin{pmatrix} \rho \\ \rho u \\ \rho v \\ \rho e \\ \rho Z \end{pmatrix} + \frac{\partial}{\partial x} \begin{pmatrix} \rho u \\ \rho u^2 + p \\ \rho uv \\ (\rho e + p)u \\ \rho Zu \end{pmatrix} + \frac{\partial}{\partial y} \begin{pmatrix} \rho v \\ \rho uv \\ \rho v^2 + p \\ (\rho e + p)v \\ \rho Zv \end{pmatrix} = \begin{pmatrix} 0 \\ 0 \\ 0 \\ 0 \\ \rho w \end{pmatrix} \quad (1)$$

The total energy  $e$  is given by

$$e = p / [\rho(\gamma - 1)] + (u^2 + v^2) / 2 - Zq \quad (2)$$

The chemical reaction is modeled by one-step irreversible reaction as follows

$$w = (1 - Z)k \exp(-E_a / RT) \quad (3)$$

The convective fluxes in Eq. (1) are integrated by the fifth-order weighted essentially non-oscillatory (WENO) scheme [12]. The discretized equations are integrated in time using a fourth-order accurate, four-stage Runge-Kutta scheme.

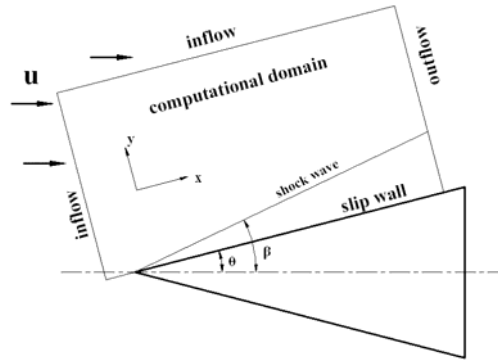


Figure 1. Schematic of the computational domain attached to the wedge surface.

Schematic of oblique detonation wave induced by the wedge is shown in Figure 1. A rectangular computational domain is considered with a dimensionless size of  $1.5 \times 0.45$ . Cartesian grid is aligned with the wedge surface and the grid numbers are  $1510 \times 450$ , which grids are fine enough to describe the detonation wave structure, since the half-reaction length is 0.013, covering 13 grid points. Ten additional cells are added upstream of the wedge surface to avoid the numerical reflection from the left boundary. Slip boundary conditions are specified at the wedge surface. Inflow conditions are fixed to the free values in both left and upper boundaries of the domain. Outflow conditions imposed to the right boundary specify zero gradients for all variables. a Mach 7 flow with  $\gamma = 1.3$  over a  $30^\circ$  wedge is treated. The heat release  $q$  and the activation energy  $E_a$  are chosen as 10 and 30, respectively.

### 3 Results and discussion

The front of oblique detonation wave induced by a wedge is composed of two different parts as shown in Figure 2, the oblique shock wave (OSW), labeled AB and the oblique detonation wave (ODW), labeled BE, where the detonation onset takes place at the intersection between OSW and ODW.

In addition, if the wedge is long enough, three regions in the flow field behind ODW can be defined following the  $x$  coordinate, i.e. section BC, CD and DE, according to the fine structures of oblique detonation as shown in Figure 2, which is a plot of pressure field of the oblique detonation structure on a  $30^\circ$  wedge in a Mach 7.0.

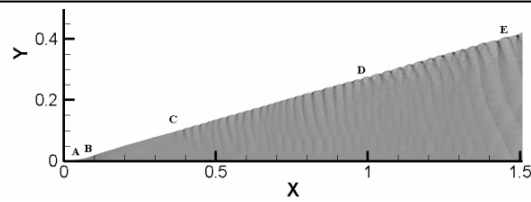


Figure 2. Pressure field of the oblique detonation structure.

In the section BC, the compression of the wedge is strong enough to make resistance to disturbances, which causes the formation of the ZND model-like detonation wave structure.

As the increase of distances from the wedge apex along the wall surface, the compression is weaker and the shock front becomes more sensitive to disturbances. Therefore, collisions between shock wavelets occur in the section CD due to disturbances, which leads to an abrupt transition from the incident shock to the oblique detonation wavelet denoted as D1 in Fig 3(b). Transverse waves emanate from collision points defined as the triple point. The close-up view of this structure in CD is shown in Fig 3, where Fig 3(a) is contours of reactive progress superimposed on the shadow pressure contour, and Fig 3(b) is a schematic diagram.

The combustible gases compressed by the shock S1 are ignited by the transverse wave and thus lead to the onset of the transverse detonation TS1. Both D1 and TS1 face upstream and move downstream due to supersonic incoming flow. As the leading shock front of D1 gradually curves downstream, its strength decreases. Finally, the decaying wave becomes a non-reactive shock wave decoupling from the reaction zone, and then will transit to a detonation again in the next cycle. All the transverse waves move downstream with almost same velocities.

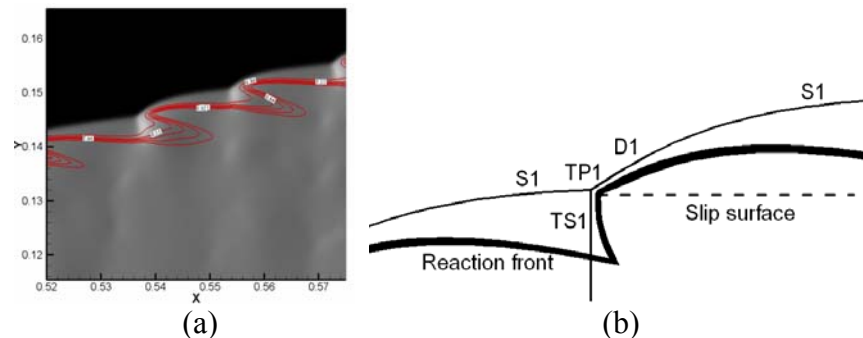


Figure 3. Close-up view of wave front structure in section CD. (a) contours of reactive progress superimposed on the shadow pressure contour (b) schematic diagram.

The oscillation feature of the detonation is also demonstrated in Fig 4, where (a) leading shock pressure history, (b) the reaction front denoted by a red line superimposed on the  $y-t$  diagram of shadow pressure distribution at a fixed location  $X_0$  in the section CD. The curve of shock pressure is periodic. At  $t=0.42$ , a triple point occurs at  $X_0$ , the pressure is highest and the shock front is coupled with the reaction. As the triple point moves downstream, the pressure decreases dramatically and then increases gradually. Meanwhile the shock front is decoupled with the reaction and then coupled gradually, till the new triple point occurs.

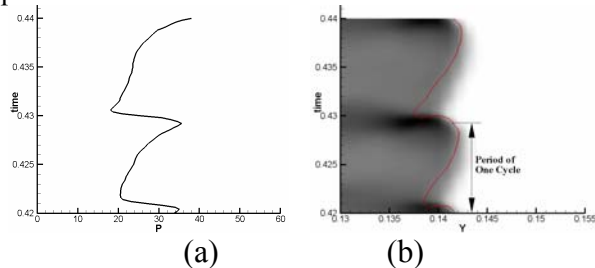


Figure 4. Oscillation feature of detonation in section CD (a) leading shock pressure history (b) reaction front superimposed on the  $y-t$  diagram of shadow pressure distribution at a fixed  $X_0$ .

In the section DE, the further distortions of shock fronts appear, so that the abrupt transition from the incident shock to the oblique detonation wavelet can happen both upstream and downstream denoted as D2 and D1 in Fig 5(b) respectively. The close-up view is shown in Fig 5. The combustible gases compressed by the shock S1 are ignited by both the transverse waves emanating from triple points TP1 and TP2 respectively, and the transverse detonations TS1 and TS2 are formed, where the incoming fresh flow penetrates into the transverse detonations TS1 and TS2 almost perpendicularly. It should also be noted that D1 and TS1 face upstream and D2 and TS2 face downstream. Based on one dimensional analysis by Yi et al [13], in a supersonic flow, the propagating velocity of the detonation facing downstream is larger than that of the detonation facing upstream, which make the triple points TP1 and TP2 move toward each other. During this process the detonation waves D1 and D2 decay gradually and become the shock wave just before the collision of triple points TP1 and TP2. Subsequent to the collision, the transverse detonations TS1 and TS2 reflect and propagate away from each other, and new detonation wavelets form. Therefore, the oscillation process of the detonation wave front has the temporal and spatial periodicity.

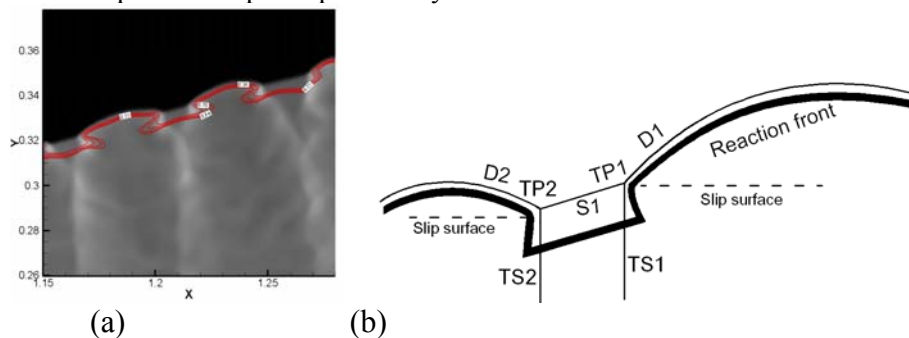


Figure 5. Close-up view of wave front structure in section DE. (a) contours of reactive progress superimposed on the shadow pressure contour (b) schematic diagram.

In order to describe this periodicity, the oscillations of detonation fronts at four fixed locations  $X_1 - X_4$ , chosen in one spatial cycle are demonstrated in Fig 6. Based on the calculations, the flow parameters on the detonation front in a temporal cycle are affected by four triple point collision events, in which the two collisions generate in the spatial cycle, denoted by subscripts  $i$  and the other collisions happen in the adjacent upstream cycle, denoted by subscripts  $u$ . Whereas superscripts  $+$  and  $-$  denote triple points TP1 and TP2 or the detonations facing upstream and downstream respectively.

At  $t=0.42$ , a triple point collision  $1_i$  just happens at the location  $X_1$ , which leads the pressure increase as shown in Fig 6(a). After the collision, the detonations facing upstream and downstream denoted as  $1^{\pm}_i$  are formed and propagate downstream with different velocities. Then, the second pressure peak  $1^-_u$  occurs in Fig 6(a), corresponding with the triple point TP2 generated in the first collision in the adjacent spatial cycle. Subsequently, the third pressure peak  $2^-_u$  occurs as the triple point TP2 generated in the second collision in the adjacent cell passes through  $X_1$ . Finally, a new temporal cycle begins, when the triple points collides again.

For other fixed locations  $X_2=X_1+\Delta X/4$ ,  $X_3=X_1+\Delta X/2$  and  $X_4=X_1+3\Delta X/4$ ,  $\Delta X$  is width of the spatial cycle, the oscillations of the detonation are shown in Fig 6(b-d) respectively. In Fig 6(b), pressure peaks  $1^{\pm}_i$  occur due to the collision at  $X_1$ . In Fig 6(c), the second triple point collision  $2_i$  occurs at the location  $X_3$  at  $t=0.426$ , and then pressure peaks  $2^{\pm}_i$  occur in Fig 6(d) due to the collision at  $X_3$ . Finally, a new spatial cycle will begin at  $X_5=X_1+\Delta X$ .

It is obvious that the oscillation feature of the detonation at a fixed location is depended on the features of the triple points passing through in a temporal cycle. Therefore the temporal oscillation patters of the detonation in a spatial cycle are different at the different locations.

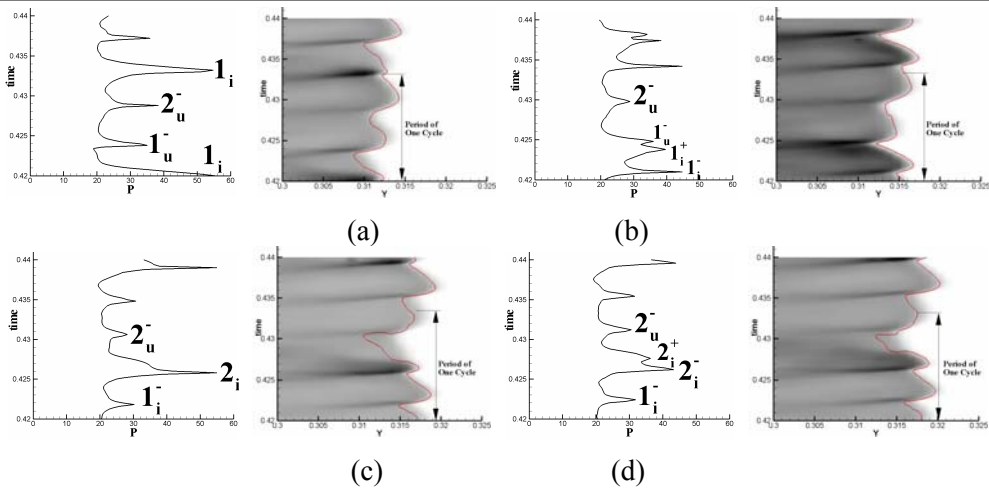


Figure 6. Oscillation feature of detonation wave at four locations in one cycle in section DE.

(a) location X1 (b) location X2 (c) location X3 (d) location X4.

Figure 7 shows variations of the instantaneous shape of the ODW front with time. The triple point traces are also drawn in this image, in which solid lines correspond to the wave facing upstream and dash lines, only appearing in DE, correspond to the wave facing downstream.

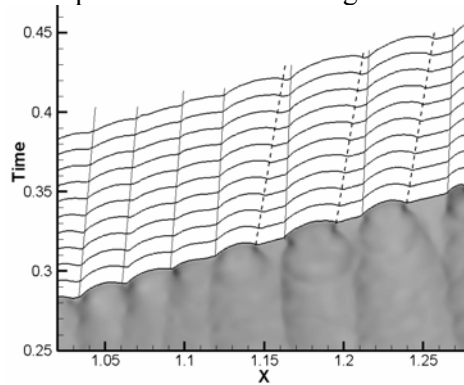


Figure 7. Variations of the instantaneous shape of the ODW front with time.

Figure 8 shows the numerical smoke-foil record. It can be observed that only set of parallel straight lines are recorded in the CD area, whereas the cellular structures are clearly seen in the DE area.

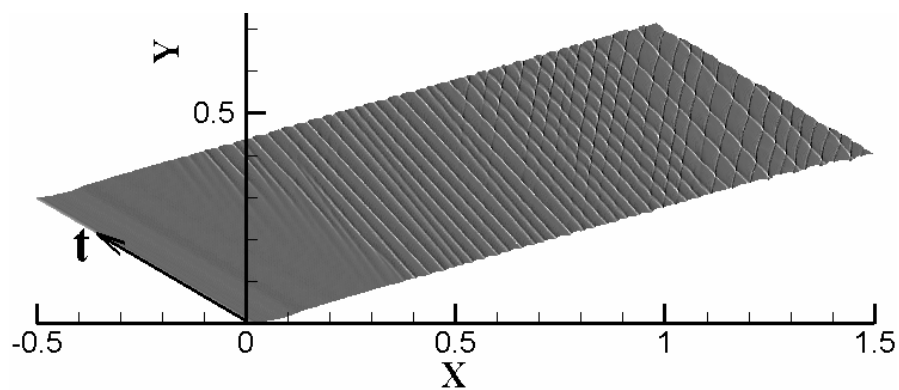


Figure 8. Numerical smoke-foil record of ODW.

### Acknowledgments

The work was supported by the natural science fund of China (No.10872096).

## References

- [1] Lehr, H. F. (1972). Experiments in shock-induced combustion. *Acta Astronaut.* 17:589-597.
- [2] Dabora, E. K., Desbordes, D., Gueraud, C., and Wagner, H. G. (1991). Oblique detonation at hypersonic velocities. *Progress in Astronautics and Aeronautics.* 133: 187-201.
- [3] Viguier, C., Gueraud, C., and Desbordes, D. (1994). H<sub>2</sub>-air and CH<sub>4</sub>-air detonations and combustions behind oblique shock waves. *Proc. Combust. Inst.* 25: 53-59.
- [4] Viguier, C., Gourara, A., and Desbordes, D. (1998). H<sub>2</sub>-air and CH<sub>4</sub>-air detonations and combustions behind oblique shock waves. *Proc. Combust. Inst.* 27: 2207-2214.
- [5] Kamel, M. R., Morris, C. I., Stouklov, I. G., and Hanson, R. K. (1996). PLIF imaging of hypersonic reactive flow around blunt bodies. *Proc. Combust. Inst.* 26: 2909-2915.
- [6] Morris, C. I., Kamel, M. R., and Hanson, R. K. (1998). Shock-induced combustion in high-speed wedge flows. *Proc. Combust. Inst.* 27: 2157-2164.
- [7] Li, C., Kailasanath, K., and Oran, E. S. (1994). Detonation structures behind oblique shocks. *Physics of Fluids.* 4: 1600-1611.
- [8] Papalexandris, M. V. (2000). A numerical study of wedge-induced detonations. *Combust. Flame.* 120: 526-538.
- [9] L. F. Figueira. da Silva., and Deshaies, B. (2000) Stabilization of an oblique detonation wave by a wedge: a parametric numerical study. *Combust. Flame.* 121: 152-166.
- [10] Choi, J. Y., Kim, D. W., Jeung, I. S. et al. (2007). Cell-like structure of unstable oblique detonation wave from high-resolution numerical simulation. *Proc. Combust. Inst.* 31: 2473-2480.
- [11] Choi, J. Y., Shin, E. J. R., Cho, D. R. et al. (2008). Onset condition of oblique detonation wave cell structures. *AIAA 2008-1032.*
- [12] Shu, C. W. (1997). Essentially non-oscillatory and weighted essentially non-oscillatory schemes for hypersonic conservation laws. *ICASE REPORT 97-65.*
- [13] Yi, T. H., Wilson, D. R., and Lu, F. K. (2004) Numerical study of unsteady detonation wave propagation in a supersonic combustion chamber. *25<sup>th</sup> International Symposium on Shock Waves.* Paper No. 10041.